Theoret. chim. Acta (Berl.) 59, 153–179 (1981)

THEORETICA CHIMICA ACTA

A CNDO/INDO Molecular Orbital Formalism for the Elements H to Br. Applications

Michael C. Böhm and Rolf Gleiter

Institut für Organische Chemie der Universität, D-6900 Heidelberg, Federal Republic of Germany

The CNDO/INDO molecular orbital formalism introduced in the preceding paper has been applied to a large number of atom combinations up to bromine under the inclusion of the first transition metal series. The results are compared with experimental data (geometries, ionization potentials, dipole moments) or with the results of sophisticated *ab initio* calculations (one electron energies, net charges, atomic populations). The semiempirical model reproduces for a wide range of molecules the experimental and *ab initio* data with remarkable success.

Key words: Semiempirical LCAO-method – CNDO- and INDO-approximation – Transition metal compounds — Computational results

1. Introduction

In the preceding paper [1] we have introduced a new parametrization for CNDO and INDO type approximations to carry out molecular orbital (MO) calculations of molecules containing atoms up to bromine. The method has been designed for any combination of atoms.

In this publication we demonstrate the capability of the method in various examples. We compare results of geometry calculations, ionization potentials and dipole moments with results of *ab initio* calculations and experiments. At the end of this paper a paragraph is included presenting results of excited states calculations on MnO_4^- and CrO_4^{2-} using restricted configuration interaction (CI).

2. Geometries

In Table 1 we have collected the calculated and experimental bond lengths of 61 diatomic molecules without a transition metal atom. As computational frame-

0040-5744/81/0059/0153/$05.40

Table 1. Calculated and experimental bond lengths of diatomic molecules (R_{xy} in Å)

X–Y	R_{XY}^{cal}	$R_{XY}^{\mathrm{exp}\ a}$	% Error	X–Y	R_{XY}^{cal}	$R_{XY}^{\mathrm{exp}\ a}$	% Error	X–Y	R_{XY}^{cal}	$R_{XY}^{\mathrm{exp}\ a}$	% Error
H_2	0.8078	0.7416	8.62	BeH^+	1.3441	1.3121	2.43	LiCl	2.0743	2.0207	2.65
Li_2	3.0675	2.6725	14.78	BeCl	1.5905	1.7000	−6.44	LiBr CNDO	2.2213	2.1704	2.34
B_2	1.4465	1.5890	−8.97	BCl	1.4961	1.7157	−12.80	LiH	1.3972	1.5935	−12.32
$C_2\ {}^1\Sigma_g^+$	1.2021	1.2422	−3.23	BF	1.2829	1.2620	1.66	MgH	1.5825	1.7306	−8.56
$C_2\ {}^3\Pi_u$	1.3246	1.3117	0.98	BBr CNDO	1.8439	1.8870	−2.28	MgH^+	1.5622	1.6490	−5.26
N_2	1.1633	1.0976	5.99	BH	1.2233	1.2325	−0.75	NaH	1.6856	1.8873	−10.69
O_2	1.2134	1.2074	0.50	BN	1.2452	1.2810	−2.79	NaBr CNDO	2.9575	2.6400	12.03
F_2	1.2043	1.4350	−16.08	BO	1.2369	1.2049	2.66	NaCl	2.3090	2.5100	−8.01
Na_2	3.3498	3.0780	8.83	ClF	1.6275	1.6281	−0.04	HF	0.8581	0.9170	−6.42
Si_2	2.2010	2.2520 [3]	−2.26	BrF CNDO	1.7778	1.7755	1.27	HCl	1.2601	1.2746	−1.14
P_2	1.6678	1.8930	−11.90	CaH	2.0497	2.0020	2.38	NO	1.1724	1.1508	1.88
S_2	1.6379	1.8870	−13.20	CaH^+	1.8641	1.7330	7.56	NH	1.0028	1.0380	−3.39
As_2 CNDO	2.4586	2.4300 [3]	1.18	CaCl	1.7793	1.8600	−4.34	OH	0.9370	0.9706	−3.46
Se_2 CNDO	2.4529	2.1570	13.72	CaF	2.2716	2.0200	12.46	PH	1.4588	1.4328	1.81
Br_2 CNDO	2.1282	2.2840	−6.82	CH	1.1377	1.1198	1.60	PN	1.4849	1.4910	−0.41
AlO	1.5017	1.6176	−7.16	CP	1.5522	1.5620	−0.63	PO	1.5355	1.4488	5.98
AlH	1.5097	1.6460	−8.28	CN	1.2040	1.1718	2.75	SiH	1.4613	1.5200	−3.86
AlCl	2.4263	2.1380	13.48	CS	1.4913	1.5344	−2.81	SiN	1.4683	1.5718	−6.58
ALBr CNDO	2.3810	2.2950	3.75	CO	1.2112	1.1281	7.37	SiS	1.9977	1.9288	3.57
BeH	1.3701	1.3122	4.42	KF	2.3520	2.5530	−7.87	SO	1.5425	1.4933	3.29
								HS	1.3418	1.3500	−0.61

[a] The experimental values are taken from [2] if not otherwise noted.

work we use the INDO approximation with the exception when the molecule contains As, Se or Br. In these cases we have to use the CNDO approach since no Slater–Condon parameters were available for these atoms.

Inspection of Table 1 shows a satisfactorily agreement between calculation and experiment with only a few exceptions. The most significant deviations from experiment we observe in those cases where very smooth potential functions are found (Li_2, AlCl, BCl, CaCl, LiH, NaBr) and in case of F_2 where all current semiempirical LCAO methods fail to predict the equilibrium geometry. Good agreement between theory and experiment is found in those diatomic molecules where both atoms X and Y have about the same electronegativity. The mean deviation in the absolute values between the calculated and experimental distance is found to be 5.6%. This value compares favourably with that found for the original INDO version (10.3%) [4] and the SINDO version (9.4%) [5].

In Table 2 the experimental determined geometrical parameters of 29 triatomic molecules of the type X_2Y and XYZ are compared with calculated ones. As in Table 1 the transition metal atoms are omitted. This comparison also shows a satisfactory agreement between experiment and calculation with an average error of about 4.6%. Again it is found that the agreement between calculation and experiment decreases with increasing difference of the electronegativity.

A similar conclusion can be drawn by comparing the experimental data with the INDO results of 42 polyatomic molecules listed in Table 3. Altogether 95 different bond lengths have been optimized. A detailed examination of the results listed, reveals some systematic errors of our method. In case of alternant π-systems (butadiene, diacetylene, propionaldehyde, furane and thiophen) the method overestimates the difference between formal double and single bonds. In case of butadiene the experimental and calculated bond lengths (in brackets) compare as follows: $R_{12} = 1.337$ Å (1.326 Å), $R_{23} = 1.476$ Å (1.574 Å). On the other hand the CC bond lengths for ethylene and ethane are given with sufficient accuracy. A comparison between experimental and theoretically predicted CC separations is given below:

ethylene

$R_{12} = 1.317$ Å theory

$R_{12} = 1.339$ Å exp.

ethane

$R_{12} = 1.487$ Å theory

$R_{12} = 1.536$ Å exp.

Another shortcoming of our INDO formalism is seen in case of single bonds between elements of the first and second period, e.g. CH_3—SH or CH_3—Cl. The calculated distances are too short. The geometrical parameters of a large number of polar systems, however, (e.g. Li_2Br_2, Li_2Cl_2, BBr_3, H_3PBH_3) are given with high accuracy.

Table 2. Calculated and experimental geometries of triatomic molecules X_2Y and XYZ, bond lengths in Å

XYZ	R_{XY}^{cal}	R_{YZ}^{cal}	$\measuredangle XYZ^{cal}$	R_{XY}^{exp} [6]	R_{YZ}^{exp}	$\measuredangle XYZ^{exp}$	% Error R_{XY}	% Error R_{YZ}
HCO	1.1395	1.2273	119.06	1.0800	1.1980	119.50	5.51	2.45
SSO	2.1774	1.5596	117.66	1.8840	1.4650	118.00	15.58	6.46
OClO	1.5572		108.25	1.4730		117.60	5.72	
NNN	1.1909		180.00	1.1850		180.00	0.50	
CNC	1.2467		180.00	1.2450		180.00	0.14	
ONO	1.1992		133.31	1.1934		134.10	0.49	
OBO	1.2839		180.00	1.2650		180.00	1.49	
NNO	1.1736	1.1282	180.00	1.1282	1.1842	180.00	4.02	1.68
OCS	1.2463	1.5317	180.00	1.1600	1.5600	180.00	7.44	−1.81
HPH	1.4533		91.98	1.4280		91.50	1.77	
ONO	1.1873		180.00	1.1850		180.00	0.19	
HNO	1.0147	1.1890	103.43	1.0630	1.2120	108.00	−4.54	−1.90
SCS	1.5298		180.00	1.5540		180.00	−1.56	
HCF	1.1492	1.2869	100.62	1.1210	1.3140	101.60	2.52	−2.06
HCCl	1.1594	1.5135	110.43	1.1200	1.6800	103.40	3.52	−9.91
HSiCl	1.4517	2.2448	107.27	1.5600	2.0640	102.80	−7.00	8.76
OOO	1.2402		114.36	1.2780		116.80	−2.96	
HSiBr[a]	1.4431	2.4204	102.85	1.5600	2.2310	102.90	−7.49	8.49
OSO	1.5670		105.18	1.4321		119.50	9.42	
OCO	1.2429		180.00	1.1621		180.00	6.95	
CCC	1.2887		180.00	1.2770		180.00	0.92	
HCP	1.1361	1.5133	180.00	1.0670	1.5420	180.00	6.48	−1.86
HSeH[a]	1.3471		119.83	1.4600		91.00	−7.73	
HBH	1.2049		131.20	1.1800		131.00	2.11	
HAlH	1.4524		120.48	1.5900		119.00	−8.65	
HOH	0.9318		128.23	0.9560		105.20	−2.53	
HSH	1.3316		102.43	1.3280		92.20	0.27	
HCN	1.1154	1.2088	180.00	1.0640	1.1560	180.00	4.83	4.56
HNH	0.9984		106.50	1.0240		103.40	−2.50	

[a] CNDO

Table 3. Calculated and experimental geometries of polyatomic molecules; bond lengths in Å

Compound	Bond lengths and bond angles, experimental values in parenthesis	% Error in bond lengths	Reference
CH_4	1.1221 (1.094)	2.57	[6]
NH_3	0.9932 (1.0173), ∡HNH = 120.00 (107.80)	−2.37	[6]
C_2H_4	CC = 1.3171 (1.339), CH = 1.1303 (1.086),	−1.63, 4.08	[6]
	∡CCH = 118.78 (120.20)		
C_2H_2	CC = 1.249 (1.208), CH = 1.1209 (1.058)	3.45, 5.95	[6]
$HSCH_3$	HS = 1.3393 (1.329), SC = 1.6173 (1.818),	0.78, −11.04	
	CH = 1.1491 (1.104), ∡HSC = 101.08 (100.30),	4.09	
	∡SCH = 111.91 (110.30)		
HCOOH	HC = 1.1492 (1.097), CO = 1.2582 (1.2020),	4.76, 4.68	[6]
	CO = 1.3150 (1.3430), OH = 0.9416 (0.9720),	−2.08, −3.12	
	∡HCO = 121.85 (124.20), ∡HCO = 119.90 (124.90),		
	∡COH = 110.78 (106.30)		
H_2CN_2	HN = 1.100 (1.08), CN = 1.2768 (1.32),	1.93, −3.27	[6]
	NN = 1.1760 (1.12), ∡HCN = 106.30 (116.50)	5.06	
Li_2Br_2	LiBr = 2.3527 (2.35), ∡LiBrLi = 106.91 (110.00)	0.11	[7]
Li_2Cl_2	LiCl = 2.2845 (2.23), ∡LiClLi = 112.96 (108.00)	2.44	[7]
$BrCH_3$[a]	BrC = 1.9527 (1.939), CH = 1.1348 (1.113),	0.71, 1.96	[6]
	∡BrCH = 107.00 (111.23)		
PH_3	1.4424 (1.421), ∡HPH = 119.20 (93.30)	1.51	[6]
HCCCOH	HC = 1.1587 (1.055), CC = 1.2505 (1.209),	9.83, 3.43	[6]
	CC = 1.5949 (1.445), CO = 1.2467 (1.214),	10.37, 2.70	
	CH = 1.1684 (1.106), ∡CCC = 91.78 (91.60),	5.65	
	∡CCO = 123.30 (120.00)		
H_3CCOH	HC = 1.1277 (1.086), CC = 1.5358 (1.501),	5.59, 2.32	[6]
	CO = 1.2532 (1.216), CH = 1.1501 (1.114),	3.06, 3.78	
	∡HCC = 105.93 (110.00), ∡CCO = 125.38 (123.90),		
	∡CCH = 123.70 (117.50)		
CNCCH	CN = 1.2109 (1.159), NC = 1.5269 (1.378),	4.48, 10.81	[6]
	CC = 1.2518 (1.205), CH = 1.1196 (1.058)	3.88, 5.82	
OBOBO	OB = 1.2524 (1.20), BO = 1.3613 (1.36),	4.37, 0.10	[7]
	∡BOB = 80.88 (95.00)		
GeH_4[a]	1.3597 (1.5270)	−10.96	[8]
AsH_3[a]	1.4699 (1.519)	−3.23	[8]
butadiene	CC = 1.3256 (1.337), CC′ = 1.5744 (1.476),	−0.86, 6.66	[6]
	∡CCC = 128.06 (122.90)		
furane	CO = 1.3342 (1.362), CC = 1.3644 (1.3610),	−2.04, 0.25	[6]
	CC′ = 1.5901 (1.431), CH = 1.1339 (1.076),	11.12, 5.38	
	∡COC = 109.67 (106.60)		
thiophene	SC = 1.6167 (1.714), CC = 1.3707 (1.3700),	−5.68, 0.05	[6]
	CC′ = 1.6013 (1.423), ∡CSC = 94.11 (92.20)	12.53	
$HCCCH_3$	HC = 1.1155 (1.056), CC = 1.2539 (1.206),	5.63, 3.97	[6]
	CC = 1.4770 (1.459), CH = 1.1281 (1.105),	1.24, 2.09	
	∡CCH = 102.15 (109.47)		
$NCCH_3$	NC = 1.2120 (1.157), CC = 1.4684 (1.458),	4.76, 0.71	[6]
	CH = 1.1278 (1.104), ∡CCH = 101.10 (109.50)	2.16	
N_2C_2	NC = 1.2107 (1.154), CC = 1.5252 (1.3890)	4.91, 9.81	[6]
HFCO	HC = 1.1462 (1.095), FC = 1.3984 (1.3380),	4.68, 4.52	[6]
	CO = 1.2501 (1.181), ∡HCO = 128.03 (127.30),	5.85	
	∡FCO = 117.94 (122.80)		

Table 3—*continued*

Compound	Bond lengths and bond angles, experimental values in parenthesis	% Error in bond lengths	Reference
ethylene oxide	CC = 1.3222 (1.427), CO = 1.5199 (1.436), CH = 1.1415 (1.082)	5.84, −7.34	[6]
$ClCH_3$	ClC = 1.5709 (1.781), CH = 1.1534 (1.113), ∡ClCH = 111.63 (109.47)	−11.80, 3.63	[6]
H_3PBH_3	HP = 1.4588 (1.399), PB = 1.7715 (1.937), BH = 1.1757 (1.212), ∡HPB = 113.55 (116.90), ∡PBH = 109.60 (103.60)	4.27, −8.55 −3.00	[7]
B_2H_6	BH = 1.4947 (1.33), BH′ = 1.3207 (1.19)	12.38, 10.98	[6]
HNO_3	HO = 0.9849 (0.9640), ON = 1.2497 (1.406), NO = 1.12305 (1.211), NO′ = 1.2157 (1.199), ∡HNO = 71.53 (102.90), ∡ONO = 104.78 (115.53), ∡ONO′ = 127.23 (113.51)	2.68, 11.12 1.61, 1.39	[7]
H_2CO	CO = 1.2452 (1.21), CH = 1.1444 (1.102), ∡HCO = 114.67 (119.45)	3.84, 2.91	[6]
H_2C_2O	HC = 1.1087 (1.08), CC = 1.3160 (1.315), CO = 1.2387 (1.16), ∡HCC = 107.64 (118.85)	2.66, 0.08 6.78	[6]
F_2CO	FC = 1.3969 (1.312), CO = 1.2601 (1.174), ∡FCO = 124.49 (126.00)	6.47, 7.33	[6]
C_2H_6	CC = 1.4867 (1.536), CH = 1.1306 (1.091), ∡CCH = 109.45 (108.00)	−3.21, 3.63	[6]
BBr_3	1.9065 (1.8932)	0.70	[7]
$AlCl_3$	2.4000 (2.06)	16.50	[7]
AlH_3	1.4590 (1.715)	−14.93	[7]
BF_3	1.4412 (1.309)	10.10	[7]
BCl_3	1.6153 (1.7421)	−7.28	[7]
$AlBr_3$[a]	2.5907 (2.44)	6.18	[7]
H_2CCCH_2	CC = 1.3129 (1.3084), CH = 1.1176 (1.0870) ∡CCH = 112.02 (120.90)	0.35, 2.82	[6]
HCCCCH	CH = 1.1197 (1.10), CC = 1.2521 (1.2055), CC = 1.5281 (1.376)	1.79, 3.87 11.05	[6]
benzene	CC = 1.4136 (1.397), CH = 1.1394 (1.084)	1.17, 5.11	[6]

[a] CNDO

With respect to bond angles also computational results of acceptable quality are predicted. Two examples with significant errors are H_2O where the INDO HOH angle of 128.23° differs by 23° from the experimental value of 105.2° and NH_3 where a planar geometry is predicted. The latter shortcoming, however, is part of most semiempirical LCAO parametrizations.

In Table 4 we have compared the predicted and experimental geometrical parameters of complex compounds of the first transition metal series. If not specifically marked the core-core interaction has been calculated according to Eq. (54) of [1]. We find a remarkable good agreement between experiment and calculation. In case of the oxo compounds MnO_4^-, CrO_4^{2-} and VO_4^{3-} the experimental and theoretical bond distances differ by less than 3%. The optimized NiC

Table 4. Calculated and experimental geometries of transition metal compounds; bond lengths in Å

Compound	Bond lengths and bond angles, experimental values in parenthesis	% Error in bond lengths	Reference
CoH	1.5331 (1.542)	-0.58	[2]
CuF	1.7720 (1.743)	1.66	[2]
MnH	1.9297 (1.7308)	11.50	[2]
CuH	1.5045 (1.463)	2.84	[2]
NiH	1.4331 (1.474)	-2.77	[2]
TiO	1.5199 (1.62)	-6.18	[2]
ZnH	1.5872 (1.5945)	-0.46	[2]
$\mathrm{ZnH^+}$	1.4026 (1.5146)	-7.39	[2]
$\mathrm{MnO_4^-}$	1.5921 (1.59)	0.13	[9]
$\mathrm{CrO_4^{2-}}$	1.6520 (1.65)	0.16	[9]
$\mathrm{VO_4^{3-}}$	1.9121 (1.86)	2.80	[9]
$\mathrm{TiCl_4}$[a]	2.1486 (2.1850)	-1.67	[10]
$\mathrm{CuCl_4^{2-}}$[a]	2.2514 (2.26)	-0.38	[11]
$\mathrm{Ni(CO)_4}$[a]	NiC = 2.0339 (1.84), CO = 1.2113 (1.15)	10.54, 5.33	[12]
$\mathrm{Ni(CN)_4^{2-}}$[a]	NiC = 1.7981 (1.86), CN = 1.2048 (1.18)	-3.33, 2.11	[13]
bis(π-allyl) nickel[a]	NiC = 1.9812 (1.98), NiC′ = 2.0620 (2.025), CC′ = 1.3777 (1.41), ∡C′NiC′ = 71.40 (74.60), ∡CC′Ni = 73.27 (67.90), CH = 1.1397, 1.1328, 1.1262	1.83, -2.29 -2.28	[14]
ferrocene[a]	FeC = 1.9959 (2.05), CC = 1.4867 (1.44), CH = 1.1385	-2.64, 3.24	[15]
$\mathrm{Fe(CO)_5}$[a]	$\mathrm{FeC_{eq}}$ = 1.8953 (1.833), $\mathrm{FeC_{ax}}$ = 1.8256 (1.806) $\mathrm{CO_{eq}}$ = 1.2179 (1.147), $\mathrm{CO_{ax}}$ = 1.2206 (1.147)	3.40, 1.09 6.18, 6.42	[16]
$\mathrm{Fe(CO)_4H_2}$[a]	$\mathrm{FeC_{eq}}$ = 1.8288 (1.80), $\mathrm{FeC_{ax}}$ = 1.7728 (1.83), $\mathrm{CO_{eq}}$ = 1.2199 (1.15), $\mathrm{CO_{ax}}$ = 1.2227 (1.15), FeH = 1.3252 (1.56)[b]	1.60, -3.12 6.08, 6.32 -15.05	[17]
$\mathrm{Co(CO)_4H}$[a]	$\mathrm{CoC_{eq}}$ = 1.8410 (1.82), $\mathrm{CoC_{ax}}$ = 1.8416 (1.76), $\mathrm{CO_{eq}}$ = 1.2165 (1.14), $\mathrm{CO_{ax}}$ = 1.2166 (1.14), CoH = 1.3000 (1.56)[b]	1.15, 4.64 6.71, 6.72 -16.67	[17]

[a] Modified core–core repulsion of Eq. (60) of Ref. [1] has been used.
[b] Bond angles were kept fixed.

distances in bis-π-allyl-nickel (1.98 and 2.06 Å) differ less than 0.04 Å from the corresponding experimental values (1.98 Å and 2.03 Å). Similarly the FeC distances calculated for ferrocene (2.00 Å) are close to the experimental value (2.05 Å). In metal-carbonyl hydride systems the metal-hydrogen distances are predicted to be too short by about 15%. The mean error between calculated and measured bond distances in Tables 1–4 amounts to 5%.

3. Ionization Potentials

One of the main goals to reparametrize the Hamiltonian for the INDO and CNDO version including transition metals was initiated by our interest in photoelectron (PE) spectroscopic investigations of transition metal-π-complexes. In various examples (ferrocene [18, 19], bis(π-allyl)nickel [20, 21], irontricarbonyl complexes [22–24]) it has been demonstrated that relaxation and correlation effects can not be neglected and thus Koopmans theorem [25] is not useful any more. To interpret PE- spectra of organometallics one is therefore forced to use methods which take into account reorganization effects during ionization. Procedures which have been successfully applied were the ΔSCF method [26, 27] and the "Transition Operator Method" (TOM) [28, 29]. In both procedures relaxation contributions are considered. If one tries to go beyond the Hartree–Fock approximation to include correlation effects, the Green's function approach [30] is the method of choice.

Since the computational effort to go beyond Koopmans' theorem is very time-consuming it seems worthwhile to test the capability of the semiempirical CNDO/INDO model in those examples where Koopmans' theorem has been shown to serve as a reasonable approximation. Thus we have collected the calculated and experimental first ionization potentials of 50 compounds in Table 5. The mean deviation between the first calculated ionization potential I_1^{cal} and the experiment, I_1^{exp}, amounts to 8.9%, a value which is significantly smaller than that found in case of Pople's INDO version (36%) [4] or the SINDO method (29%) [5]. In Fig. 1 we have plotted I_1^{cal} as a function of I_1^{exp}. The linear relation between both is determined by eq. (1):

$$I_1^{\mathrm{cal}} = 2.13 + 0.87\, I_1^{\mathrm{exp}}. \tag{1}$$

The standard deviation is 0.79 eV, the regression coefficient is calculated to be 0.92. These results show that our CNDO/INDO model allows a satisfactory interpretation of PE spectroscopic data. A further improvement is found if the calculated ionization potentials are based on the experimental geometries and not on the optimized ones. A comparison between the data of Table 5 with that of Tables 1–3 clearly displays that the deviation in ionization potentials parallels the deviation in geometrical parameters.

In part I we discussed in some detail the shortcomings of current semiempirical LCAO procedures (MINDO/3, CNDO/2, EHT) to predict the separations

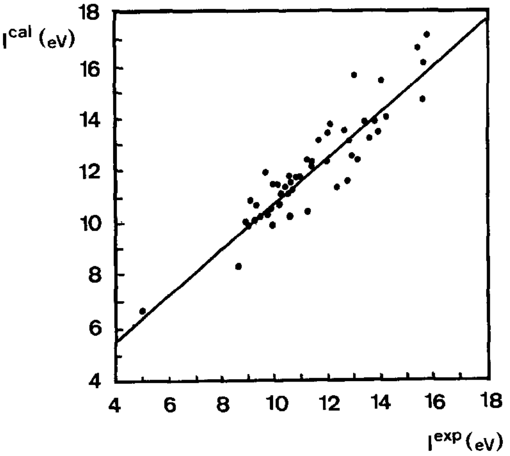

Fig. 1. Graphical correlation between the calculated (I^{cal}) and measured (I^{exp}) first vertical ionization potentials

Table 5. Comparison between the calculated (I_1^{cal}) and measured (I_1^{exp}) first ionization potentials. All values in eV

Compound	I_1^{cal}	I_1^{exp}	% Error	Reference
H_2	16.68	15.43	8.10	[31]
Li_2	6.71	4.96	35.28	[31]
C_2	13.42	12.00	11.83	[31]
N_2	14.68	15.58	−5.78	[31]
O_2	13.75	12.08	13.82	[31]
F_2	16.13	15.70	2.74	[31]
CN	14.09	14.20	−0.77	[31]
CO	15.41	14.01	9.99	[31]
NO	10.65	9.27	14.89	[31]
HF	17.17	15.77	8.88	[31]
OH	13.84	13.36	3.59	[31]
NH	12.41	13.10	−5.27	[31]
CH	11.25	10.64	5.73	[31]
BH	10.28	9.70	5.98	[31]
BeH	8.33	8.60	−3.14	[31]
HCl	11.58	12.73	−9.03	[32]
HCO	11.45	9.88	15.89	[6]
N_2O	12.55	12.89	−2.64	[6]
OCS	12.39	11.24	10.23	[6]
CS_2	11.45	10.08	13.59	[6]
O_3	13.14	12.80	2.66	[6]
SO_2	11.36	12.34	−7.94	[6]
CO_2	13.84	13.77	0.51	[6]
BH_2	10.49	9.80	7.04	[6]
H_2O	13.52	12.62	7.13	[6]
H_2S	11.10	10.47	6.02	[6]
HCN	13.46	13.91	−3.24	[6]
H_2N	12.16	11.40	6.67	[6]
CH_4	15.62	12.99	20.25	[6]
NH_3	10.66	10.15	5.02	[6]
C_2H_4	11.78	10.51	12.08	[6]
C_2H_2	12.35	11.41	8.24	[6]
$HSCH_3$	10.23	9.44	8.37	[6]
HCOOH	12.18	11.33	7.50	[6]
H_2CN_2	9.90	9.00	10.00	[6]
$BrCH_3$	10.22	10.54	−3.04	[6]
H_2CO	11.75	10.88	8.00	[6]
H_2CCO	11.90	9.61	16.44	[6]
C_2H_6	13.13	11.65	12.70	[6]
H_2CCCH_2	11.10	10.19	8.93	[6]
HCCCCH	11.71	10.79	8.53	[6]
$HCCCH_3$	11.35	10.36	9.56	[6]
NCCN	13.21	13.57	−2.65	[6]
ethylene oxide	11.55	10.57	9.27	[6]
$ClCH_3$	10.41	11.22	−7.22	[6]
benzene	10.10	9.25	10.27	[6]
butadiene	10.83	9.06	19.54	[6]
furane	10.04	8.89	12.94	[6]
thiophene	9.99	8.85	12.88	[6]
$NCCH_3$	12.33	11.95	3.18	[6]

Table 6. Comparison between measured vertical ionization potentials, $I_{v,j}$, of the hydrocarbons 1, 2, 3, 4 and 5 and calculated orbital energies by means of INDO and MINDO/3; all values in eV

Compound	$I_{v,j}$	Assignment	INDO	MINDO/3
1	8.41	π_A	−10.33	−8.96
	10.20	π_S	−11.34	−10.45
	10.70	σ	−11.55	−10.01
2	8.48	π_A	−10.41	−8.90
	9.02	π_{bridge}	−10.61	−9.00
	10.35	π_S	−11.39	−10.44
	11.29	σ	−11.79	−10.40
3	7.69	π_A	−9.76	−8.60
	9.68	π_S	−10.27	−9.80
	10.64	σ	−10.79	−9.67
4	8.06	π_A	−9.78	−8.61
	8.90	π_{bridge}	−9.84	−8.96
	9.85	π_S	−10.60	−9.96
	10.50	σ	−10.86	−9.73
5	7.90	π_A	−9.70	−8.57
	9.10	π_{bridge}	−9.81	−9.18
	10.01	π_S	−10.65	−9.94
	10.30	σ	−10.93	−9.90

between π and σ MO's which follow from PE spectroscopic studies. Usually the σ-orbitals are placed at too high energies. A semiempirical model transferring this drawback to transition metal compounds would be of little help as the MO sequence of a complex depends on the interaction strengths and energy difference of all the fragment orbitals.

To demonstrate the validity of our INDO model we present in Table 6 measured and calculated ionization potentials (INDO and MINDO/3) of the strained hydrocarbons **1** to **5** with high lying σ-orbitals [33]. For the interpretation of the

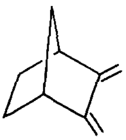

1

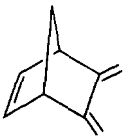

2

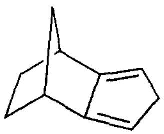

3

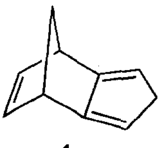

4

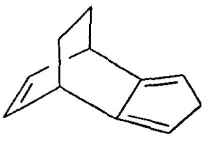

5

Table 7. Comparison between measured vertical ionization potentials ($I_{v,j}^{\exp}$)of two Fe transition metal tricarbonyl derivatives with ΔSCF and TOM results($I_{v,j}^{\Delta\mathrm{SCF}}$, $I_{v,j}^{\mathrm{TOM}}$)based on the INDO Hamiltonian and ΔSCF *ab initio* findings derived on the near minimal-basis level; all values in eV

Compound	$I_{v,j}^{\exp}$	Γj	$I_{v,j}^{\Delta\mathrm{SCF}}$ INDO	$I_{v,j}^{\mathrm{TOM}}$ INDO	$I_{v,j}^{\Delta\mathrm{SCF}}$ *ab initio*
6	8.45	$30a'$	8.18	7.07	8.4
		$16a''$	8.60	7.03	8.5
		$29a'$	8.75	7.40	—
	9.21	$17a''$	8.93	8.58	8.1
		$31a'$	8.98	8.63	8.2
7	8.62	$17a_1$	8.64	7.82	8.2
		$14e$	8.85	7.61	8.5
	9.26	$15e$	9.64	9.17	8.4
	11.07	$16a_1$	11.77	11.30	13.3

PE spectra the validity of Koopmans' theorem ($I_{v,j} = \varepsilon_j$) [25] has been assumed. The experiment clearly shows [33] that the π-orbitals are placed on top of the σ-orbitals for all five examples. The gap between π and σ-orbitals is between 0.3 and 0.9 eV. The comparison in Table 6 shows that the experimental sequence is only reproduced by INDO while MINDO/3 always interchances π_S and σ. As in the case of the examples collected in Table 5 the ionization potentials derived from our INDO model and values based on Koopmans' theorem show a mean shift to negative values of about 1 eV. Taking into account relaxation and correlation effects by means of a Greens function many-body approach [30] the difference between $I_{v,j}$ and the INDO based on ionization potentials is significantly reduced by about 0.5–0.8 eV, typical for Koopmans' defects of organic compounds. These examples demonstrate that our INDO parametrization avoids failures which are part of existing semiempirical LCAO models.

Recently we have used our semiempirical INDO Hamiltonian to calculate ionization potentials in the outer valence region of transition metal compounds. In Table 7 we show a comparison between our results using the transition operator method (TOM) as well as the ΔSCF procedure based on our INDO Hamiltonian [34] and the results of a ΔSCF calculation using a near minimal basis *ab initio* calculation for irontricarbonyl-cyclobutadiene (**6**) [23] and irontricarbonyl-trimethylenemethane (**7**) [24].

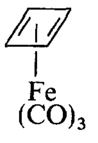

6

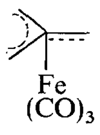

7

Table 8. Comparison between measured vertical ionization potentials ($I_{v,j}^{exp}$) of the various transition metal species **8**–**10** with ΔSCF and TOM results ($I_{v,j}^{\Delta SCF}$ $I_{v,j}^{TOM}$) based on the INDO Hamiltonian; all values in eV

Compound	$I_{v,j}^{exp}$	MO	MO-Type	$I_{v,j}^{\Delta SCF}$	$I_{v,j}^{TOM}$
8	7.3	38	Fe $3d_{x^2-y^2}/3d_{xy}$	7.26	6.37
		37	Fe $3d_{x^2-y^2}/3d_{xy}$	7.35	6.43
	8.3	36	Fe $3d_{xy}/3d_{yz}$	7.88	7.21
		35	Fe $3d_{xy}/3d_{yz}$	7.78	6.81
	10.8	34	FeC-σ	11.48	11.28
	11.5	33	π-OCO group	11.53	11.77
	12.3	31	$n_{\ominus}$ lone-pair	12.74	12.54
9	7.1	44	Fe $3d_{x^2-y^2}$	6.61	5.82
	7.3	43	Fe $3d_{xy}$	6.97	6.08
	8.3	41	Fe $3d_{yz}$	7.32	6.63
		40	Fe $3d_{xz}$	7.17	6.36
	8.7	42	π, NCN group	8.54	8.01
	10.8	39	FeC-σ	10.21	10.13
10	6.95	27 ($10a_1$)	Fe $3d_{x^2-y^2}$	7.16	6.53
	7.80	31 ($8b_1$)	Fe $3d_{xz}$, L(π*)	7.51	7.10
	8.25	26 ($6b_2$)	Fe $3d_{yz}$, L(π)	7.63	6.95
		30 ($11a_1$)	Fe $3d_{z^2}$, L(π*)	7.97	7.45
	9.15	29 ($7b_2$)	L(π)	9.26	8.62
	9.55	28 ($5a_2$)	L(π)	10.00	9.74

L(π) ≡ ligand-π

The first band in the PE spectra of both compounds is due to ionization events out of molecular orbitals with predominant Fe 3*d* character, while the remaining bands correspond to ligand orbitals. It is seen that the *ab initio* approach completely fails to reproduce the experimental splitting between metal 3*d* and ligand bands. On the other hand the energy gap between both types of ionization events is well reproduced by the relaxation methods (ΔSCF, TOM) based on the INDO-Hamiltonian. The capability of the semiempirical method is also recognized on the basis of Table 8 where we have compared measured and calculated (ΔSCF, TOM) ionization potentials of the ironcarbonyl compounds **8**–**10** [35, 36].

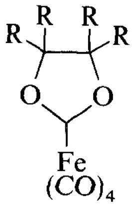

8

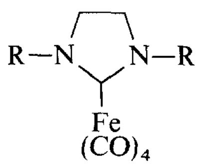

9

$R = CH_3$

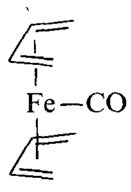

10

Table 9. The lowest ligand IP and Ni $3d$ IP of bis(π-allyl)nickel compared with INDO results based on the Greens function approach and ΔSCF *ab initio* calculations; all values in eV

		INDO Greens Function		*ab initio* near minimal basis ΔSCF		*ab initio* double-zeta	
Type	$I^{\exp}_{v,j}$	$I_{v,j}$	Γj	$I_{v,j}$	Γj	$I_{v,j}$	Γj
L(π)	7.76	8.75	$7a_u$	8.92	$7a_u$	7.30	$7a_u$
Ni $3d$	8.19	8.91	$13a_g$	7.92	$9a_g$	5.71	$9a_g$

L(π) ≡ ligand (π).

Once again the separation between the various ionization events originating from the metal and ligand orbitals is given with remarkable accuracy.

Table 9 collects the lowest ionization potentials of bis(π-allyl)nickel as derived by means of a many-body approach based on the Green's function within the INDO model [37] and ΔSCF *ab initio* results within a near minimal basis [20] and double zeta basis set [21]. The experimental sequence ligand-π on top of Ni $3d$ has been derived unequivocally by means of extensive experimental informations (e.g. band intensities, alkyl-induced shifts, exchange of Ni against Pd and Pt) [38]. It is seen that the experimental sequence is only reproduced within the INDO-based Greens function approach. On the other hand both *ab initio* calculations predict a different sequence of ionization events. Within the near minimal basis approximation an inverted sequence is calculated that differs by 1.4 eV from the experiment. This error is enlarged to 2.0 eV in the case of the extended basis. Thus it seems that ΔSCF *ab initio* calculations are of limited value for the prediction of vertical ionization potentials of organometallics in the outer valence region because the neglect of electron correlation leads to dramatical errors. On the other hand it should be noticed that the Greens function procedure based on INDO results leads to an entire assignment of the PE spectrum of bis(π-allyl)-nickel in the outer valence region with a standard deviation between measured and calculated ionization potentials of 0.08 eV and a regression coefficient of 0.9989 [37].

4. Dipole Moments

The quality of calculated charge distributions can be tested by comparing calculated and observed dipole moments. Very often dipole moments are poorly reproduced and average errors between theory and experiment span a range between 40 and 50% [4, 5]. In Table 10 we have collected various examples between calculated and experimenatl dipole moments of various ionic and covalent molecules excluding transition metal compounds. The 24 examples show an average error of 25% which is about the half of that obtained by other semiempirical methods. The dipole moments were calculated at the optimized INDO geometries.

Table 10. Calculated and experimental dipole moments (in debye); INDO-model

Compound	Calculated	Experimental	% Error	Reference
OH	2.49	1.65	50.91	[31]
HF	2.66	1.82	46.15	[31]
NaCl	5.16	8.50	−39.29	[39]
NaBr[a]	9.40	9.40	0.00	[39]
LiH	6.58	5.88	11.90	[31]
LiBr[a]	7.24	6.25	15.84	[39]
LiCl	7.33	8.20	−10.61	[39]
KF	9.84	7.33	34.24	[39]
CH	2.19	1.46	50.00	[31]
BrF[a]	2.14	1.29	65.89	[39]
ClF	1.07	0.88	21.59	[39]
HCN	2.76	2.95	−6.44	[39]
H_2O	2.29	1.84	24.46	[39]
OCS	0.79	0.73	8.22	[39]
HCOOH	2.05	1.76	20.59	[39]
$BrCH_3$[a]	1.85	1.79	3.35	[39]
H_2CO	3.46	2.17	59.45	[39]
H_2CCO	1.61	1.31	22.90	[39]
$H_3C{-}CN$	3.19	3.92	−18.62	[39]
ethylene oxide	2.13	1.88	18.62	[39]
H_3CCl	1.99	1.94	2.58	[39]
$CN{-}C{\equiv}CH$	2.94	3.60	−18.33	[39]
ethyleneimine	2.32	1.89	22.75	[39]

[a] CNDO.

Since experimental data are lacking in case of transition metal compounds we only list one example below [40] which had been investigated spectroscopically by us.

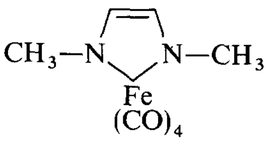

$\mu_{cal} = 7.99$ D

$\mu_{exp} = 6.59$ D

5. Comparison of Calculated Orbital Energies with Those of *ab initio* Calculations for Transition Metal Systems

In Table 11 and Fig. 2 we compare the orbital energies resulting from our INDO model with the results of three different *ab initio* calculations carried out by Johansen [41], Wood [42] and Connor et al. [43] together with the X_α calculation of Johnson and Smith [44] on MnO_4^-. The Gaussian type basis of Johansen is near the Hartree–Fock accuracy, the (16, 13, 6|10, 6) basis set was contracted to [10, 7, 3|5, 3]. The corresponding basis sets of Wood were: (12, 8, 6|8, 5) contracted to [5, 4, 3|3, 2]. The basis of Connor et al. is slightly better than a minimal basis set.

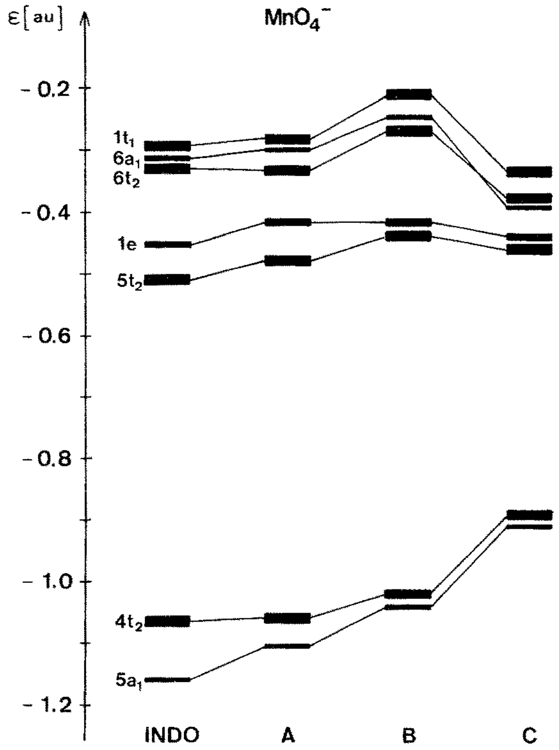

Fig. 2. Comparison of the orbital energies, ε_i, of MnO_4^- according to the INDO Hamiltonian with *ab initio* results of Johansen (A), Connor and Hillier (B) and the X_α energies of Johnson and Smith (C)

Inspection of Table 11 clearly demonstrates the good agreement between the INDO orbital energies and the one-electron eigenvalues of Johansen. The average error between $\varepsilon_{\mathrm{INDO}}$ and the near Hartree–Fock *ab initio* energies summed over the occupied valence orbitals is 5%. The comparison between the orbital energies obtained by the minimal basis set and the X_α results on one side and Johnson's approach differ by 11.6 and 16% respectively. From Table 11 and Fig. 2 it is clearly seen that especially the energy gap between the various groups of valence orbitals is reproduced by INDO with high accuracy: The MO's $5a_1$ and $4t_2$ (predominantly of oxygen $2s$ type) are separated by 0.59 au (0.61 au with *ab initio*) from the $5t_2$ and $1e$ group, the well known 3d MO's of a tetrahedron. On top of these MO's the group consisting of $6t_2$, $6a_1$ and $1t_1$ is found. These are valence orbitals predominantly of oxygen $2p$ character. In case of the virtual orbitals, e.g. $7t_2$, $2e$, $7a_1$ and $8t_2$, significant differences are found among the various calculational procedures. The computer time used to calculate MnO_4^- with INDO was 8 sec on a IBM 370/168.

In Table 12 and Fig. 3 the orbital energies of $Ni(CO)_4$ obtained by our INDO method, an *ab initio* calculation [45] and a recent CNDO extension to the first transition metal series [46] are compared. The Gaussian basis for $Ni(CO)_4$ was (12, 8, 5|8, 4|8, 4) contracted to [5, 4, 2|3, 2|2, 1]. The agreement between INDO and *ab initio* results is satisfactory over the entire valence region. The outcome of

Table 11. Orbital energies of *ab initio* and INDO calculations on MnO_4^-. Orbital energies in au

MO	Johansen [41]	Wood [42]	Connor [43]	Johnson Smith [44]	INDO	% Error
valence orbitals						
$5a_1$	−1.103	−1.080	−1.041	−0.906	−1.155	4.71
$4t_2$	−1.082	−1.060	−1.020	−0.893	−1.086	0.37
$5t_2$	−0.471	−0.475	−0.438	−0.457	−0.505	7.22
$1e$	−0.422	−0.441	−0.418	−0.450	−0.452	7.11
$6t_2$	−0.333	−0.339	−0.268	−0.381	−0.323	−3.00
$6a_1$	−0.295	−0.305	−0.244	−0.387	−0.308	4.41
$1t_1$	−0.280	−0.283	−0.211	−0.341	−0.301	7.50
virt. orbitals						
$7t_2$	0.200	0.183		−0.175	0.202	
$2e$	0.202	0.164		−0.263	0.036	
$7a_1$	0.318	0.213		−0.003	0.747	
$8t_2$	0.488	0.213		−0.010	0.511	

both methods shows perfect conformity concerning the energy of the ligand orbitals, small differences, however, occur in the case of the Ni $3d$ valence MO's $2e$ ($3d_{x^2-y^2}$, $3d_{z^2}$) and $9t_2$ ($3d_{xz}$, $3d_{yz}$, $3d_{xy}$). This difference is due to the limitation on single-zeta functions for the semiempirical MO model, a shortcoming that can not perfectly be compensated for by more sophisticated parametrization schemes. Summed over the 11 valence orbitals the deviation between the *ab initio* and INDO results is 6.4%.

A comparison of the one-electron energies obtained for $Ni(CO)_4$ with the CNDO, INDO and *ab initio* method (Table 12 Fig. 3) reveals that the energy difference

Table 12. Orbital energies of *ab initio* and semiempirical (CNDO and INDO) calculations on $Ni(CO)_4$. All values in au

MO	*ab initio* [45]	CNDO [46]	% Error CNDO [46]	INDO	% Error INDO
$5t_2$	−1.530	−1.689	10.39	−1.498	−2.09
$6a_1$	−1.530	−1.675	9.48	−1.522	−0.52
$7a_1$	−0.809	−1.222	38.69	−0.824	1.85
$6t_2$	−0.793	−0.922	16.25	−0.721	−9.08
$8a_1$	−0.693	−0.828	19.48	−0.707	2.02
$1e$	−0.665	−0.820	23.31	−0.620	−6.77
$7t_2$	−0.662	−0.815	23.11	−0.636	−3.93
$1t_1$	−0.653	−0.780	19.45	−0.598	−8.42
$8t_2$	−0.644	−0.689	6.99	−0.563	−12.58
$2e$	−0.471	−0.419	−11.04	−0.393	−16.56
$9t_2$	−0.395	−0.330	−16.46	−0.368	−6.84

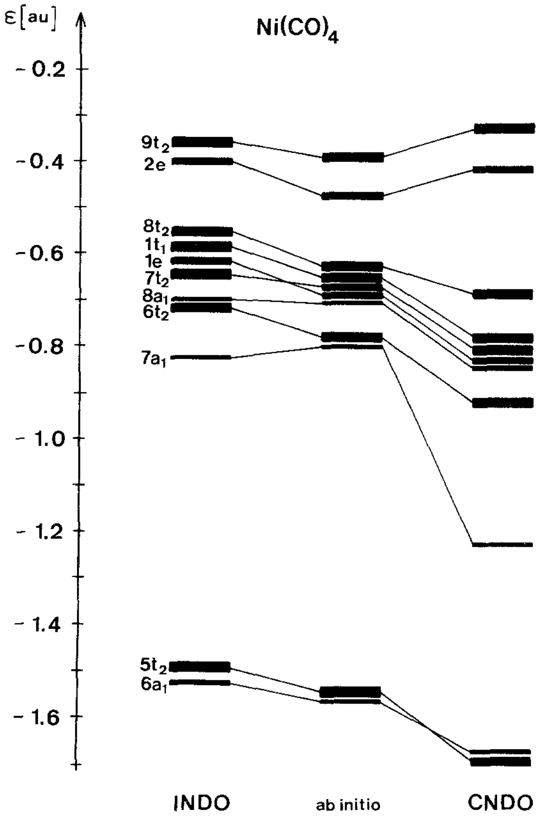

Fig. 3. Comparison of the orbital energies, ε_i, of Ni(CO)$_4$ according, to the present INDO model (left) with *ab initio* results of Demuynck and Veillard (middle) and CNDO data of Freund and Hohlneicher (right)

between ligand MO's and Ni 3d levels is conserved in the INDO case while there is a considerable imbalance between both types of orbitals in the CNDO case. This is mainly due to the fact that for non-metal atoms the parameters originally suggested by Pople [47] have been used in the CNDO-version and only new parameters were taken for the transition metal. Hence the one-electron energies of MO's predominantly localized at the ligand site are predicted at rather low energies. Thus the calculation of ionization potentials of those organometallic compounds for which the ligand MO's and metal $3d$ orbitals are close in energy is difficult and will lead to errors. This shortcoming of the CNDO method is avoided in case of our INDO model which is not based on the original CNDO/INDO version but is newly parameterized for all elements.

Recently a very accurate *ab initio* calculation on HCo(CO)$_4$ has been published [48]. In Table 13 and Fig. 4 the one-electron energies for the valence orbitals are compared with the results of our INDO model. With few exceptions (mostly in case of MO's of symmetry a_1) the agreement between both procedures is satisfactory. It should be noted that the energy gap between MO's mainly localized at the ligand side and the predominantly $3d$ MO's $11e$ ($3d_{xz}$, $3d_{yz}$) and $12e$ ($3d_{xy}$, $3d_{x^2-y^2}$), is reproduced within the semiempirical model. The difference

Table 13. Orbital energies of *ab initio* and INDO calculations on $HCo(CO)_4$. All values in au

MO	*ab initio* [48]	INDO	% Error
$12a_1$	−0.8377	−0.9007	7.52
$13a_1$	−0.8051	−0.7365	−8.52
$6e$	−0.7947	−0.7227	−9.06
$14a_1$	−0.7947	−0.7098	−1.55
$7e$	−0.6929	−0.6597	−4.97
$8e$	−0.6649	−0.6249	−6.02
$15a_1$	−0.6633	−0.6701	1.03
$9e$	−0.6552	−0.6066	−7.42
$1a_2$	−0.6507	−0.6030	−7.33
$10e$	−0.6443	−0.5798	−10.01
$16a_1$	−0.6323	−0.5545	−12.30
$11e$	−0.5286	−0.4361	−17.50
$12e$	−0.3927	−0.3986	1.50
$17a_1$	−0.3901	−0.4206	7.82

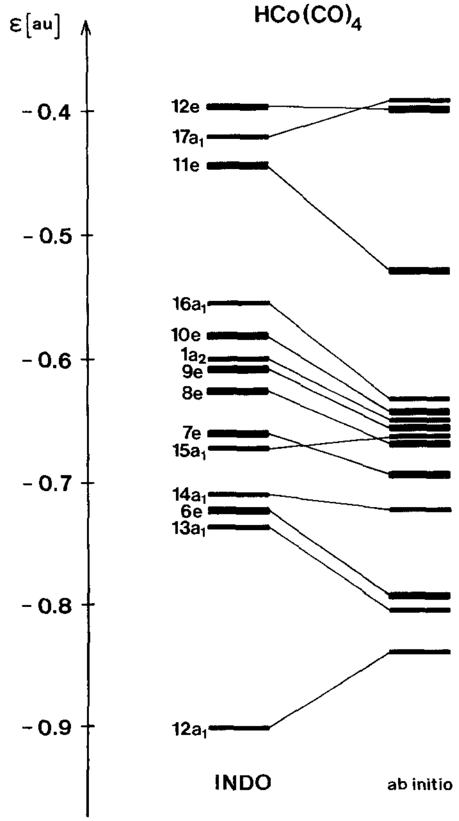

Fig. 4. Comparison of the orbital energies, ε_i, of $HCo(CO)_4$ according to the INDO method with *ab initio* eigenvalues

Table 14. Orbital energies of *ab initio* and INDO calculations on bis(π-allyl)nickel. All values in au

MO	*ab initio* [21]	INDO	% Error
$3b_g$	−0.636	−0.620	−2.52
$5a_u$	−0.613	−0.616	0.49
$9a_g$	−0.598	−0.531	−11.20
$10a_g$	−0.561	−0.525	−6.42
$4b_g$	−0.554	−0.529	−4.51
$10b_u$	−0.545	−0.518	−4.95
$6a_u$	−0.541	−0.512	−5.36
$11a_g$	−0.524	−0.460	−12.21
$5b_g$	−0.516	−0.459	−11.05
$12a_g$	−0.512	−0.457	−10.74
$11b_u$	−0.449	−0.420	−6.46
$13a_g$	−0.435	−0.410	−5.75
$6b_g$	−0.327	−0.406	24.16
$7a_u$	−0.288	−0.335	16.32

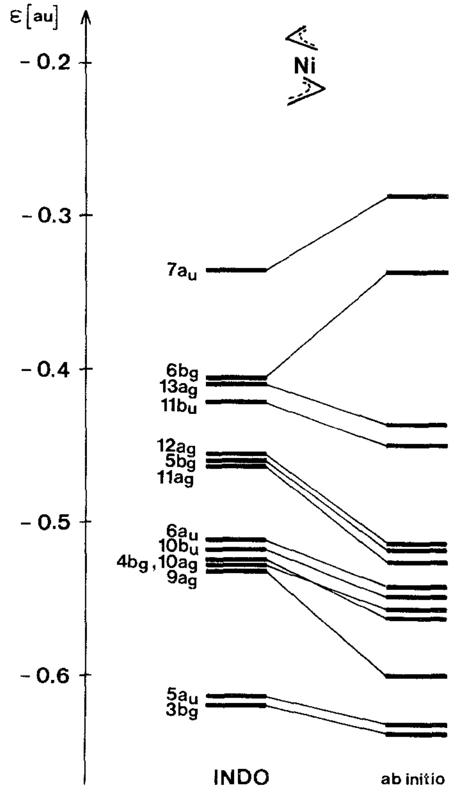

Fig. 5. Comparison of the orbital energies, ε_i, of bis(π-allyl)nickel according to the INDO model with *ab initio* results

between the INDO and *ab initio* eigenvalues is 7.3% if one takes into account the whole valence region from $12a_1$ to $17a_1$.

In Table 14 and Fig. 5 double-zeta type *ab initio* results for bis(π-allyl)nickel [21] are opposed to the corresponding INDO energies. Again there is a close correspondence between both results. With the exception of the two topmost molecular orbitals $6b_g$ and $7a_u$ there is a linear shift of about 0.05 au (= 1.16 eV) between the *ab initio* and INDO results. The average error between both one-electron energies is less than 9%. As a last example showing the efficiency of the INDO method we compare in Table 15 the molecular orbital energies of CrO_4^{2-} and VO_4^{3-} obtained by an *ab initio* calculation of near double-zeta quality [43] with the INDO results. Inspection of the Table 15 demonstrates that also in case of highly charged species the orbital sequence is reproduced and the absolute values are close to the ones obtained by the *ab initio* method.

With the last five examples we have demonstrated that our INDO model is capable to reproduce orbital energies of high quality *ab initio* calculations with sufficient accuracy. The average energy difference between the results of both methods is about 7% in the valence region which amounts to 1–1.5 eV. In every example the relative energy gap between MO's predominantly localized at the metal side and those localized at the ligands is mimicked by the INDO compared to *ab initio* results. This similarity is an important prerequisite for the explicit calculation of the ionic states of these compounds.

6. Population Analysis

A very sensitive test for the quality of semiempirical results are the resulting populations and net charges. Below we compare the results of a population analysis according to Mulliken [49] for the samples discussed already. In Table 16 some representative values for MnO_4^- are given. The first two columns list the results of Johansen with two different basis sets [41] in column three the near double-zeta values of Connor et al. [43] are shown. In column four the corresponding INDO values are listed. It is seen that the $3d$ population of Mn predicted by INDO corresponds close to the values obtained from a large basis set calculation. The $4s$, $4p$ population, however, resembles more the values of the double-zeta basis. The calculated Mn net charge of 1.604 is in line with traditional concepts which estimate the charge of Mn in MnO_4^- of about +2. The results obtained for CrO_4^{2-} and VO_4^{3-} (Table 17) are similarly close to *ab initio* findings. The only difference is due to the $4p$ occupation which is slightly underestimated by the semiempirical approach. Due to this difference a more pronounced charge drift to the oxygen $2p$ functions is calculated.

In Table 18 a detailed comparison of *ab initio* and INDO populations is given for $Ni(CO)_4$ [45]. The net charge predicted for Ni is similar with both methods. In the case of the carbonyl ligands *ab initio* predicts stronger charge separation between C and O than INDO. In comparison with the free ligand INDO predicts a

Table 15. Orbital energies of *ab initio* and INDO calculations on CrO_4^{2-} and VO_4^{3-}. All values in au

ε_i	ε_i *ab initio* [43]	INDO
CrO_4^{2-}		
$5a_1$	−0.7358	−0.8474
$4t_2$	−0.7139	−0.8490
$5t_2$	−0.1086	−0.2651
$1e$	−0.0991	−0.1989
$6a_1$	0.0127	−0.0390
$6t_2$	0.0157	−0.0546
$1t_1$	0.0809	−0.0377
VO_4^{3-}		
$5a_1$	−0.4735	−0.4325
$4t_2$	−0.4584	−0.4243
$5t_2$	0.1830	0.4065
$1e$	0.1940	0.1249
$6a_1$	0.2207	0.2550
$6t_2$	0.2504	0.1943
$1t_1$	0.3244	0.1981

significant charge transfer to the C-atoms. The charges predicted for the free ligand are +0.19 (C) and −0.19 (O).

The comparison between INDO and *ab initio* results for bis(π-allyl)nickel shows a very close agreement also concerning the outcome of a population analysis (Table 19).

The difference in charge at the Ni is due to the difference in $4s$, $4p$ population as noticed in the other examples. Both methods predict a comparable amount of

Table 16. Comparison of calculated net charges of MnO_4^-

	Johansen [41]				
	Mn	16/13/6	14/10/5	Connor/Hillier	
	0	10/6	7/3	et al. [42]	INDO
Mn	$4s$	0.328	0.332	0.147	0.102
	$4p$	0.747	0.857	0.515	0.200
	$3d$	4.948	4.697	5.448	5.094
net charge		+0.986	+1.114	+0.93	+1.604
O	$2s$	1.908	1.945	1.909	1.905
	$2p$	4.589	4.584	4.573	4.747
net charge		−0.497	−0.529	−0.48	−0.651

Table 17. Comparison of calculated net charges of CrO_4^{2-} and VO_4^{3-}

		ab initio [43]	INDO
CrO_4^{2-}	Cr		
	4*s*	0.1987	0.1264
	4*p*	0.8204	0.3345
	3*d*	4.4312	4.4250
	net charge	+0.58	+1.1141
	O		
	2*s*	1.8650	1.8730
	2*p*	4.7819	4.9055
	net charge	−0.64	−0.7785
VO_4^{3-}	V		
	4*s*	0.3224	0.2503
	4*p*	1.1945	0.6093
	3*d*	3.5712	3.5495
	net charge	−0.07	+0.5909
	O		
	2*s*	1.8418	1.8198
	2*p*	4.8917	5.0779
	net charge	−0.73	−0.8977

Table 18. Comparison of calculated net charges of $Ni(CO)_4$

		ab initio [45]	INDO
Ni	4*s*	−0.02	0.05
	$4p_x$	0.19	0.02
	$4p_y$	0.19	0.02
	$4p_z$	0.19	0.02
	$3d_{x^2-y^2}$	1.81	1.91
	$3d_{xy}$	1.90	1.91
	$3d_{xz}$	1.81	1.91
	$3d_{yz}$	1.81	1.91
	$3d_{z^2}$	1.90	1.91
net charge		+0.24	+0.37
C	2*s*	1.53	1.81
	2*p*	2.17	2.17
net charge		+0.29	+0.02
O	2*s*	1.79	1.85
	2*p*	4.56	4.26
net charge		−0.35	−0.11

Table 19. Comparison of calculated net charges of bis (π-allyl) nickel

		ab initio [21]	INDO
Ni	$4s$	0.11	0.05
	$4p_x$	0.11	0.02
	$4p_y$	0.05	0.02
	$4p_z$	0.12	0.03
	$3d_{x^2-y^2}$	1.93	1.94
	$3d_{xy}$	1.86	1.82
	$3d_{xz}$	1.15	1.37
	$3d_{yz}$	1.99	1.98
	$3d_{z^2}$	2.03	2.00
net charge		+0.65	+0.78
C_1	$2s$	1.48	1.05
	$2p$	2.86	3.01
net charge		−0.33	−0.06
C_2	$2s$	1.30	1.13
	$2p$	3.08	3.38
net charge		−0.38	−0.51

charge transfer between ligand and metal, they differ, however, with respect to the charge distribution in the ligand. *Ab initio* predicts a comparable electron excess for all three C atoms while the INDO model localizes the surplus of electron density at the terminal C atoms.

Finally in Table 20 we have listed the populations for ferrocene as derived by a minimal basis set calculation except for the $3d$ functions for Fe [18] and the INDO outcome. The differences encountered are somewhat larger: The charge at the Fe differs by 0.8.

The comparisons given in Tables 16 to 20 demonstrate that the INDO all valence procedure predicts charge distributions that are in good agreement with the results of *ab initio* calculations and corresponds to empirical ideas based on electronegativity considerations.

7. Excited State Properties

To test the INDO version upon its capability to reproduce the energies of excited states of transition metal compounds we performed a 9×9 CI calculation for MnO_4^- and CrO_4^{2-}. In Table 21 the INDO results on MnO_4^- are compared with experimental values [50–52].

The agreement between theory and experiment is very good in case of the first two transitions, but less for bands three and four. In case of CrO_4^{2-} (Table 22) the

Table 20. Comparison of calculated net charges of ferrocene

	ab initio [18]	INDO
Fe		
$4s$	0.00	0.09
$4p_x/p_y$	0.24	0.08
$4p_z$	0.01	0.06
$3d_{xz}/d_{yz}$	0.43	0.81
$3d_{xy}/d_{x^2-y^2}$	1.86	1.87
$3d_{z^2}$	1.93	1.99
net charge	+1.23	+0.42
C		
$2s$	1.12	1.06
$2p$	3.19	3.11
net charge	−0.31	−0.17
H		
$1s$	0.81	0.87
net charge	+0.19	+0.13

Table 21. Calculated singlet excited states and experimental transition energies of MnO_4^-

Experiment state excitation energy (eV)	INDO excitation energy (eV)	Oscillator strength	Orbital transition
$^1T_1$ 1.80	1.94	0.0000	$1t_1 \rightarrow 2e$ (97%)
$^1T_2$ 2.30	2.34	0.0022	$1t_1 \rightarrow 2e$ (58%) $6t_2 \rightarrow 2e$ (42%)
$^1T_2$ 3.00–3.70	4.30	0.1349	$6t_2 \rightarrow 2e$ (47%) $1t_1 \rightarrow 2e$ (32%)
$^1T_2$ 3.99	5.96	<0.0001	$1t_1 \rightarrow 7t_2$ (65%)

Table 22. Calculated singlet excited states and experimental transition energies of CrO_4^{2-}

Experiment state excitation energy (eV)	INDO excitation energy (eV)	Oscillator strength	Orbital transition
$^1T_1$ 2.80	3.28	0.0000	$1t_1 \rightarrow 2e$ (97%)
$^1T_2$ 3.20	3.61	0.0026	$1t_1 \rightarrow 2e$ (56%) $6t_2 \rightarrow 2e$ (44%)
$^1T_2$ 4.60	5.35	0.1683	$6t_2 \rightarrow 2e$ (46%) $1t_1 \rightarrow 2e$ (34%)
$^1T_2$ 6.20	6.49	0.0020	$1t_1 \rightarrow 7t_2$ (77%)
$^1T_2$ 6.90	6.57	0.0119	$6t_2 \rightarrow 7t_2$ (79%)

agreement between experiment [53, 54] and calculation is better with the exception of the third band observed at 4.6 eV.

8. Conclusions

In the last six paragraphs we have compared the results of a newly parameterized CNDO/INDO version either with experimental data or results of sophisticated *ab initio* calculations. The comparison is very satisfactory and concludes that our CNDO/INDO model can serve as a powerful tool to predict the electronic properties of a large variety of molecules of large size where methods based on first principles can not be applied.

The low computational cost of our CNDO/INDO extension to transition metal compounds is clearly seen in the synopsis of used computer times on an IBM 370/168 (in sec.).

$NiCl_2$	2
MnO_4^-	8
$Ni(CO)_4$	30
$Ni(C_3H_5)_2$	45
$Fe(CO)_5$	50
$Cr(CO)_6$	70
ferrocene	100
dibenzol chromium	150
triple-decker sandwich compounds (e.g. $Ni_2Cp_3^+$)	500–800
biferrocene	700
bis-biphenyl-dichromium	1000

Hence CNDO/INDO calculations on nearly all organometallics of general interest are possible without limitations due to computer time and computational storage, two factors that strongly restrict the use of extended basis set *ab initio* calculations in the case of complex transition metal compounds.

Furthermore we have shown that it is possible to get insight into the failures of Koopmans' theorem in the case of organometallics via various approaches that take into account relaxation and correlation effects. Here it even has been demonstrated that a properly designed semiempirical effective Hamiltonian exceeds the predictive capability of an *ab initio* Hamiltonian with a AO basis that does not reach the HF limit.

It can not be expected that our NDO extension reaches the accuracy and capability of Dewars semiempirical LCAO versions (MINDO/3 [55], MNDO [56]) where the parameters were determined by means of least square procedures for selected atom combinations. This desirable strategy is prevented in our case due to the number of different atoms and due to missing experimental data for complex and organometallic compounds.

Since our CNDO/INDO Hamiltonian has been parameterized to mimic results of *ab initio* ground state calculations it is anticipated that the results of excited state calculations reveal more pronounced deviations from the experiment.

Acknowledgement. We are grateful for financial support by the Deutsche Forschungsgemeinschaft, the Fonds der Chemischen Industrie and the BASF Ludwigshafen. This is part 13 in the series "Electronic Structure of Organometallic Compounds". Part 12 see Ref. [1].

References

1. Böhm, M. C., Gleiter, R.: Theoret. Chim. Acta (Berl.).
2. Herzberg, G.: Spectra of diatomic molecules. Princeton: Van Nostrand 1950
3. Tables of Interatomic Distances and configurations in Molecules and Ions, Special Publication No. 18, The Chemical Society, London 1965
4. Pople, J. A., Beveridge, D. L., Dobosh, P. A.: J. Chem. Phys. **47**, 2026 (1967)
5. Coffey, P., Jug, K.: J. Am. Chem. Soc. **95**, 7575 (1973)
6. Herzberg, G.: Electronic spectra of polyatomic molecules. New York: Van Nostrand 1966
7. Hargittai, M., Hargittai, I.: The Molecular Geometries of Coordination Compounds in the Vapour Phase. Amsterdam: Elsevier 1977
8. Hase, H. L., Schweig, A.: Theoret. Chim. Acta (Berl.) **31**, 215 (1973)
9. Special Publication No. 11, The Chemical Society, London 1958; Sutton, L. E., Ed.
10. Kimura, M., Kimura, K., Akai, M., Shibata, S.: Bull. Chem. Soc. (Japan) **29**, 95 (1956)
11. Willett, R. D.: J. Chem. Phys. **41**, 2243 (1964); Helmholtz, L., Kruh, R. F.: J. Am. Chem. Soc. **74**, 1176 (1952)
12. Ladell, J., Post, B., Faukuchen, I.: Acta Cryst. **5**, 795 (1952)
13. Holt, E. M., Watson, K. J.: Acta Chem. Scand. **23**, 14 (1969)
14. Bond lengths and bond angles are taken from an X-ray investigation on bis(π-methallyl)nickel: Uttech, R., Dietrich, H.: Z. Kristallogr. **122**, 60 (1965)
15. Haaland, A., Nilsson, J. E.: Acta Chem. Scand., **22**, 2653 (1968)
16. Almenningen, A., Haaland, A., Wahl, K.: Acta Chem. Scand. **23**, 2245 (1969)
17. McNeill, E. A., Scholer, F. R.: J. Am. Chem. Soc. **99**, 6243 (1977)
18. Coutière, M.-M., Demuynck, J., Veillard, A.: Theoret. Chim. Acta (Berl.) **27**, 281 (1972)
19. Bagus, P. S., Wahlgren, U. I., Almlöf, J.: J. Chem. Phys. **64**, 2324 (1976)
20. Rohmer, M.-M., Veillard, A.: J. C. S. Chem. Commun. 250 (1973)
21. Rohmer, M.-M., Demuynck, J., Veillard, A.: Theoret. Chim. Acta (Berl.) **36**, 93 (1974)
22. Connor, J. A., Derrick, L. M. R., Hall, M. B., Hillier, I. H., Guest, M. F., Higginson, R. B., Lloyd, D. R.: Mol. Phys. **28**, 1193 (1974)
23. Hall, M. B., Hillier, I. H., Connor, J. A., Guest, M. F., Lloyd, D. R.: Mol. Phys. **30**, 839 (1975)
24. Connor, J. A., Derrick, L. M. R., Hillier, I. H., Guest, M. F., Lloyd, D. R.: Mol. Phys. **31**, 23 (1976)
25. Koopmans, T.: Physica **1**, 104 (1934)
26. Bagus, P. S.: Phys. Rev. **139**, 1619 (1965)
27. Moser, C. M., Nesbet, R. K., Verhaegen, G.: Chem. Phys. Letters **12**, 230 (1971)
28. Goscinski, O., Pickup, B. T., Purvis, G.: Chem. Phys. Letters **22**, 167 (1973)
29. Firsht, D., Pickup, B. T.: Chem. Phys. Letters **56**, 295 (1978)
30. Cederbaum, L. S., Domcke, W.: Adv. Chem. Phys. **36**, 205 (1977)
31. Pople, J. A., Beveridge, D. L.: Approximate molecular orbital theory. New York: McGraw-Hill 1970
32. Turner, D. W., Baker, C., Baker, A. D., Brundle, C. R.: Molecular photoelectron spectroscopy. London: Butterworth 1974
33. Böhm, M. C., Carr, R. V. C., Gleiter, R., Paquette, L. A.: J. Am. Chem. Soc. **102**, 7218 (1980)
34. Böhm, M. C., Gleiter, R.: J. Comput. Chem. **1**, 407 (1980)

35. Böhm, M. C., Daub, J., Gleiter, R., Hofmann, P., Lappert, M. F., Öfele, K.: Chem. Ber. **113**, 3629 (1980)
36. Böhm, M. C., Gleiter, R.: Chem. Ber. **113**, 3647 (1980)
37. Böhm, M. C., Gleiter, R.: Theoret. Chim. Acta (Berl.) **57**, 315 (1980)
38. Böhm, M. C., Gleiter, R., Batich, C. D.: Helv. Chim. Acta **63**, 990 (1980)
39. McClellan, A. L.: Tables of experimental dipole moments. San Francisco: W. H. Freeman & Co. 1963
40. Öfele, K., Kreiter, C. G.: Chem. Ber. **105**, 529 (1972)
41. Johansen, H.: Chem. Phys. Letters **17**, 569 (1972)
42. Wood, M. H.: Theoret. Chim. Acta (Berl.) **36**, 309 (1975)
43. Connor, J. A., Hillier, I. H., Saunders, V. R., Wood, M. H., Barber, M.: Mol. Phys. **24**, 492 (1972)
44. Johnson, K. H., Smith Jr., F. C.: Chem. Phys. Letters **10**, 219 (1971)
45. Demuynck, J., Veillard, A.: Theoret. Chim. Acta (Berl.) **28**, 241 (1973)
46. Freund, H. J., Hohlneicher, G.: Theoret. Chim. Acta (Berl.) **51**, 145 (1979)
47. Pople, J. A., Segal, G. A.: Chem. Phys. **44**, 3289 (1966)
48. Fonnesbech, N., Hjortkjaer, J., Johansen, H.: Intern. J. Quantum Chem. **12**, Suppl. **2**, 95 (1977)
49. Mulliken, R. S.: J. Chem. Phys. **23**, 1833 (1955); **23**, 2443 (1955)
50. Teltow, J.: Z. Phys. Chem. B **40**, 397 (1938); B **43**, 198 (1939)
51. Holt, L. S., Ballhausen, C. J.: Theoret. Chim. Acta (Berl.) **7**, 313 (1967)
52. Mullen, P., Schwochau, K., Jørgensen, C. K.: Chem. Phys. Letters, **3**, 49 (1969)
53. v. Halban, H., Litmanowitsch, M.: Helv. Chim. Acta **24**, 44 (1941)
54. Johnson, L. W., McGlynn, S. P.: Chem. Phys. Letters **7**, 618 (1970)
55. Bingham, R. C., Dewar, M. J. S., Lo, D. H.: J. Am. Chem. Soc. **97**, 1285 (1975)
56. Dewar, M. J. S., Thiel, W.: J. Am. Chem. Soc. **99**, 4899 (1977)

Received September 15, 1980/December 29, 1980